Electronic Supplementary Material (ESI) for Nanoscale.

SUPPORTING INFORMATION for

Graphene dispersions in alkanes: toward fast drying conducting inks

A. Al Shboul, C. Trudeau, S. Cloutier, M. Siaj* and J. P. Claverie*

Table of Content

Confocal Raman microscopy

The graphitization degree was confirmed by Raman spectroscopy using a Confocal Raman Microscope (CRM, Alpha300 R, Witec, Germany) equipped with a 532nm class 3B laser having a spatial resolution in the x-y axis of 0.25 um and 0.5um in the z axis. The raw Raman data were processed using Witec software. Background and cosmic ray subtraction were performed to create identical baseline for each spectra and to remove spikes present due to cosmic rays hitting the spectrometer. Analysis of the Raman peaks were performed with the help of numerical filters. Two such filters were used: sum filters and gaussian filters. The sum filter acts as an integrator and sums the intensities of each bin within the given range (for example the start and end of the G peak), whereas the gaussian filter fits a gaussian curve to the data within a given range. All Raman data were processed and compared with these filters for each of the flakes edge and basal plane is indicated in table S1. In general Gauss filters tend to give lower D/G ratios, as the filter minimize the high S/N regions which are at the base of the peak. $(\Gamma/\Gamma_s)\%$ is the percentage of surface coverage of the graphene flake by the polymer determined by normalizing the surface coverage by the specific surface of graphene taken at 2630 m^2/g.[1]**.** In confocal Raman microscopy, graphene leaflets are first located by optical microscopy which has not a high enough resolution to image the smallest graphene flakes. Thus, the size of the flakes measured by confocal Raman microscopy is larger than the size of the flakes measured by AFM.

Table S1 Average I_D/I_G for the edge and center of the graphene flakes convoluted with the instrument functions nonlinear filters; Gauss fit and sum signal filters.

Polymer	Sum filter		Gauss filter		
(mg.mL^{-1})	I_D/I_G Edge	I_D/I_G Center	I_D/I_G Edge	I_D/I_G Center	$(\Gamma/\Gamma s)\%$
0	0.17	0.12	0.14	0.08	--------
0.5	0.40	0.29	0.28	0.19	23
1	0.54	0.43	0.37	0.28	65
2	0.63	0.49	0.46	0.35	80
4	0.28	0.22	0.20	0.15	86
6	0.33	0.19	0.21	0.13	75

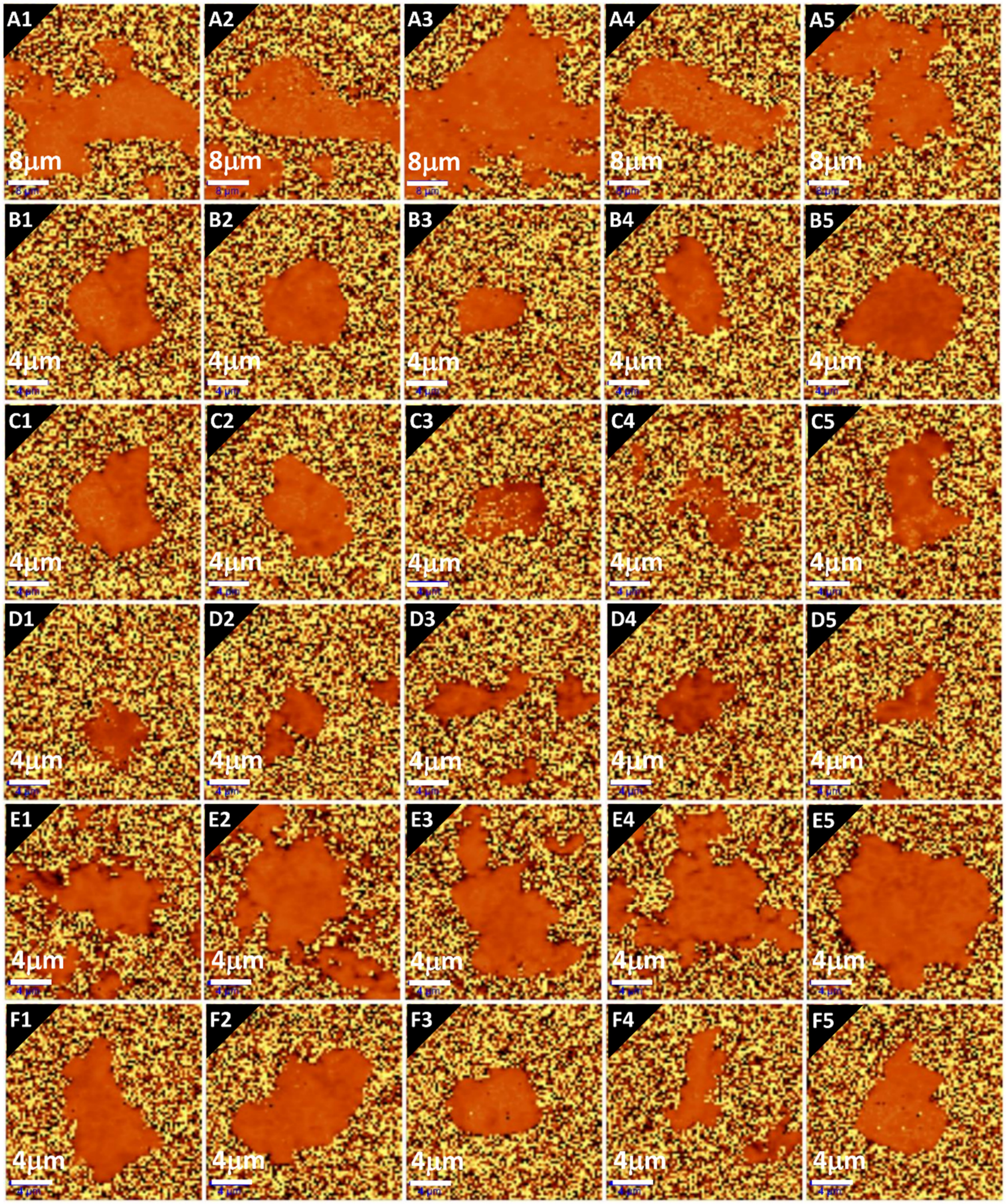

Figure S1 Raman images of graphite (A (1-5)) and of graphene flakes (B-F (1-5)). Graphene flakes were prepared with different polymer concentrations B(1-5) 0.5 mg.mL^{-1}, C(1-5) 1 mg.mL^{-1}, D(1-5) 2 mg.mL^{-1}, E(1-5) 4 mg.mL^{-1}, F(1-5) 6 mg.mL^{-1}. All the images have been treated the Gaussian filter and are color-coded according to D/G ratio

X-ray photoelectron spectrometry (XPS)

Samples for XPS were prepared by depositing a few drops of the graphene dispersions on silicon wafer. Once dried, the excess polymer was removed by immersing the slides in pure hexane for a few minutes. In order to calibrate the spectrum, the carbon peak was set at 285 eV. The quality of the sp^2 domains and chemical change in the graphitic structure was confirmed by XPS, as shown in Figure S2. In XPS, The C 1s signals of the graphene can be deconvoluted into three signals indicating different types of bonds, namely the C=C bond in aromatic rings (285.0 eV), C-O bond (285.5 eV) and C=O bond (286.5 eV).[2,3] The intensity of the C=C peak decreases and the one of the C-O and C=O peaks increases with increasing polymer concentrations indicating that C-O and C=O peaks originate from the polymer.

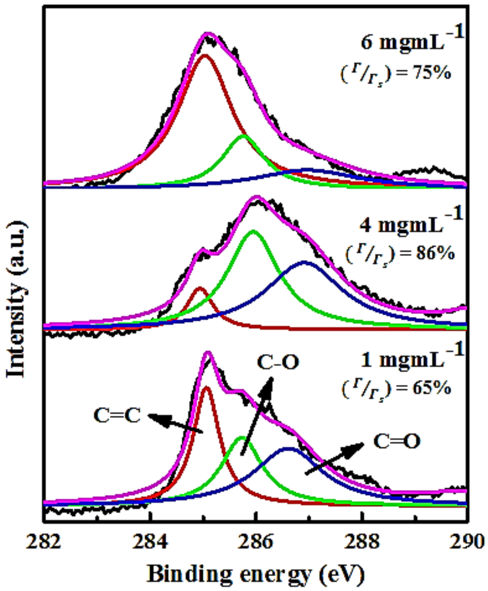

Figure S2 C 1s XPS spectra of graphene dispersion at different polymer concentration (a) 1.0 (b) 4.0 (c) 6.0 mg.mL^{-1}, and deconvolution in C=C (red), C-C (blue) and C-O (green) peaks.

Atomic Force Microscopy (AFM)

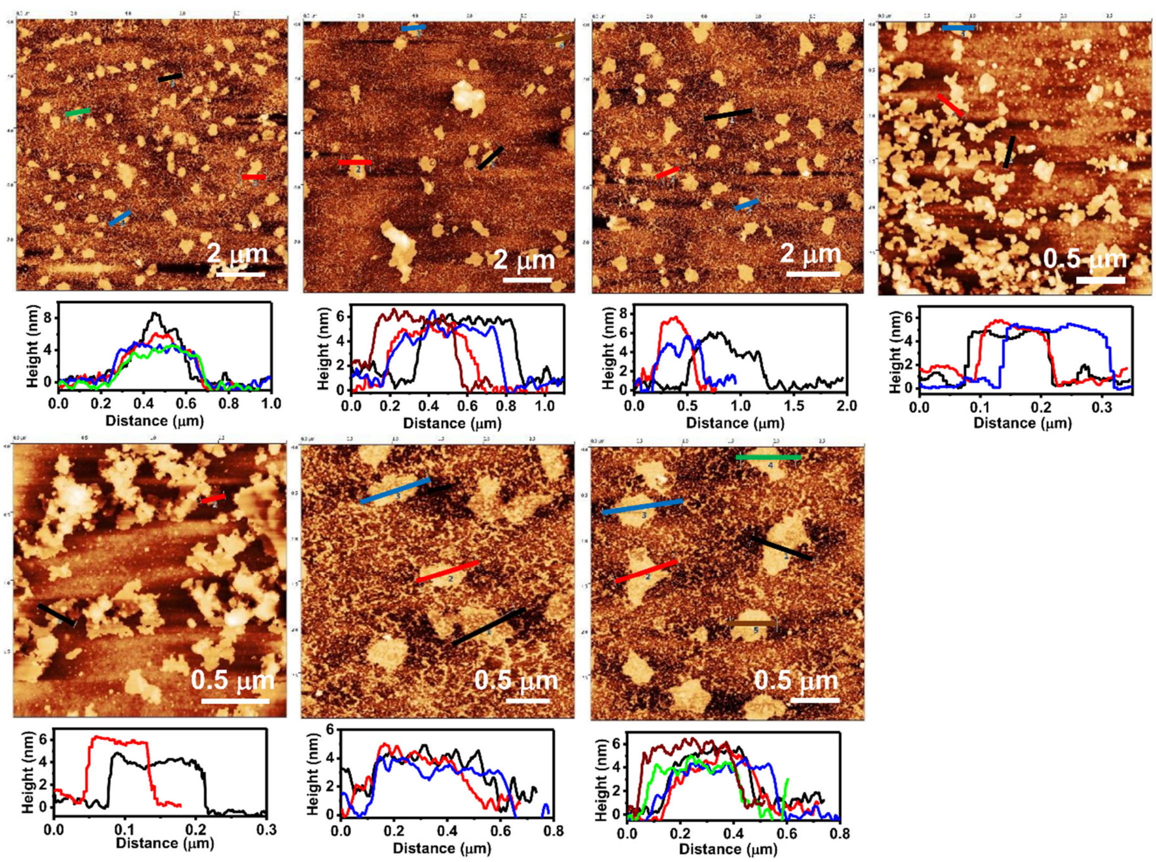

Figure S3 AFM images of graphene flakes before removing the unbound polymer.

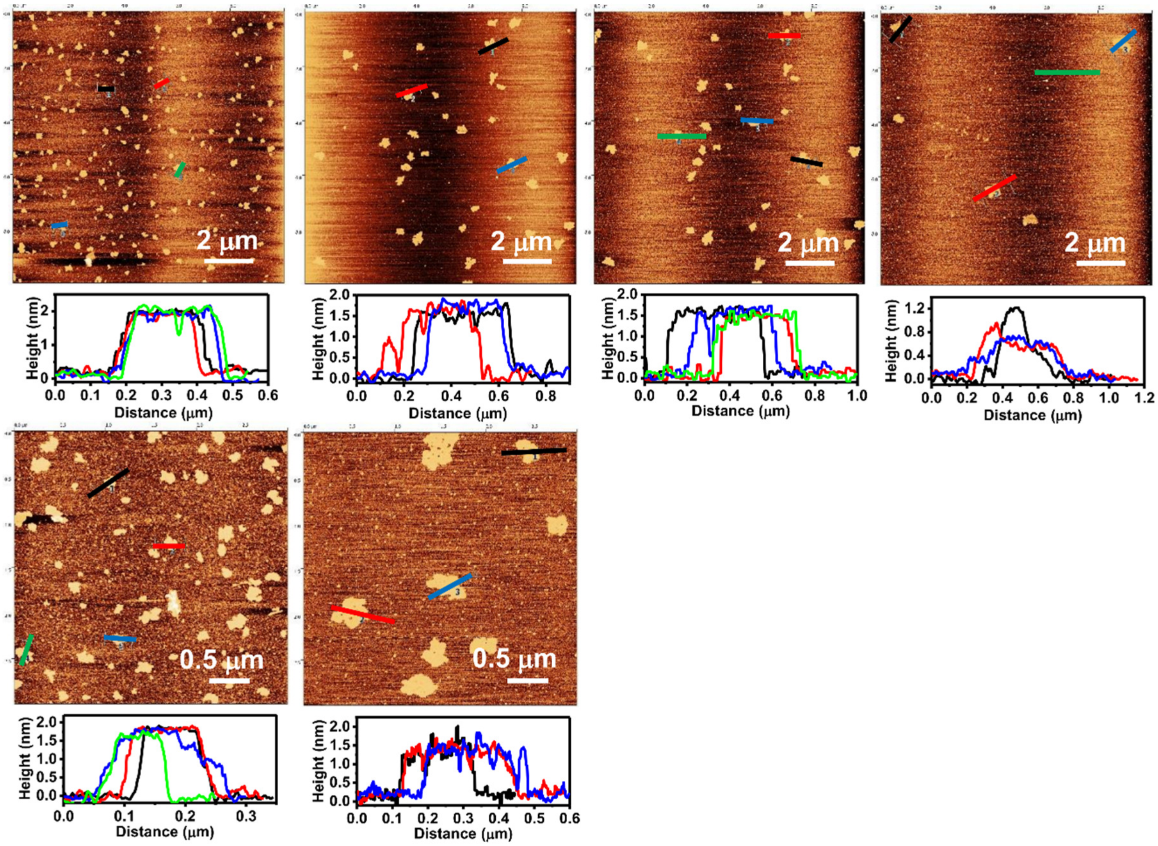

Figure S4 AFM images of graphene flakes prepared after removing the unbound polymer.

Scanning Electron Microscopy (SEM)

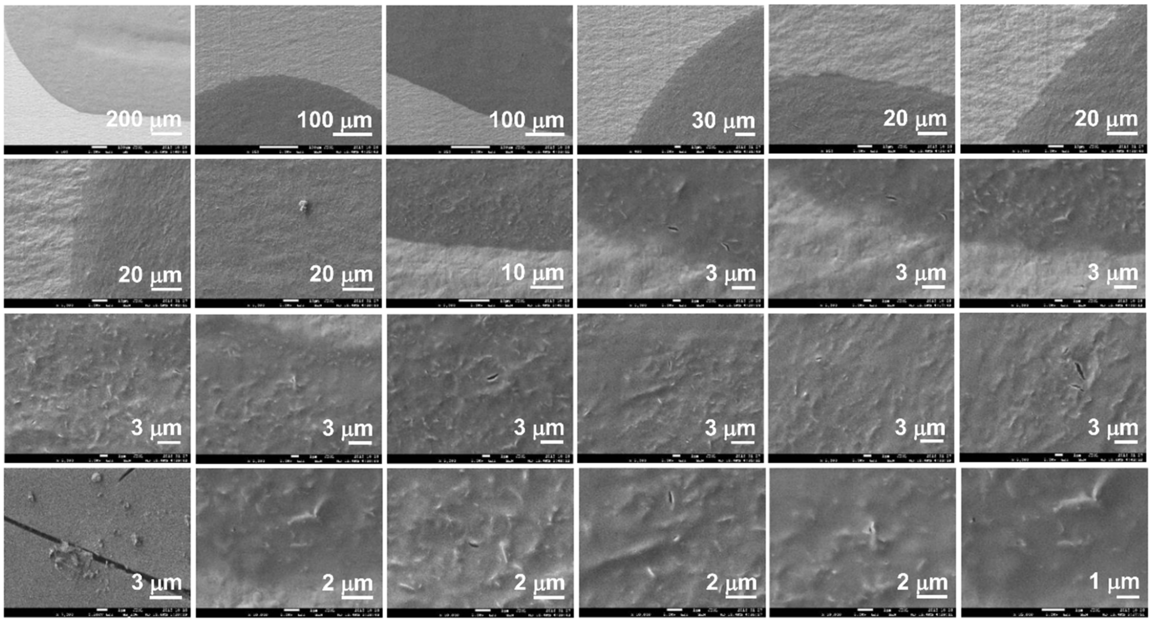

Figure S5 SEM images of the films prepared with graphene inks (0.5 mg.mL^{-1}, $\Gamma/\Gamma_s = 23\%$) written with a ballpoint pen on aluminum foil.

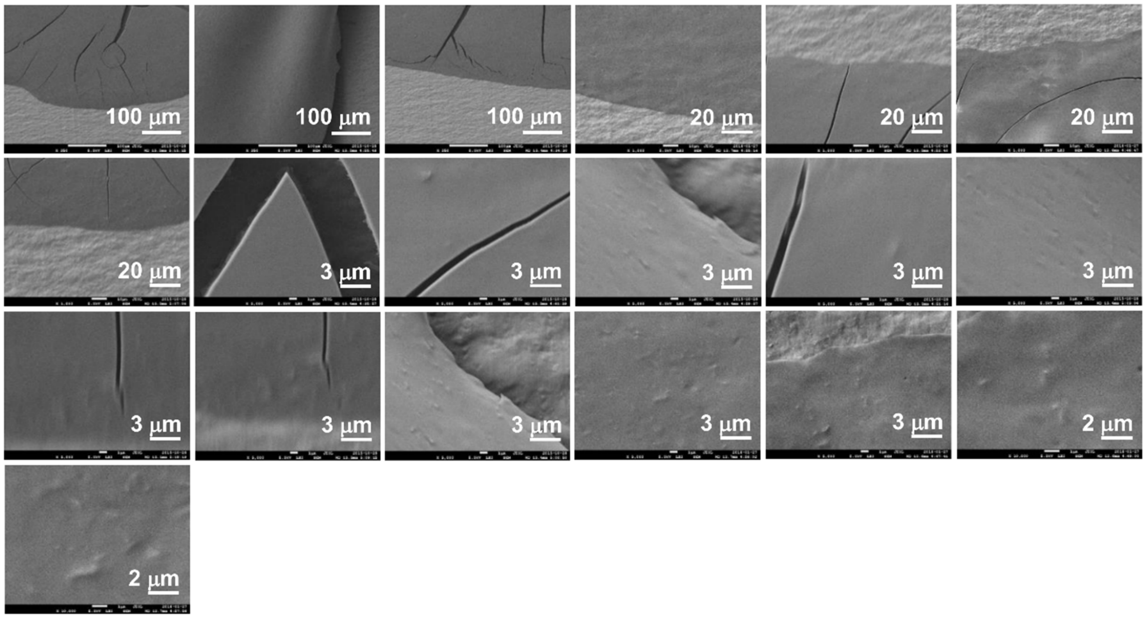

Figure S6 SEM images of the films prepared with graphene inks (1 mg.mL^{-1}, Γ/Γ_s = 65%), written with a ballpoint pen on glass on aluminum foil.

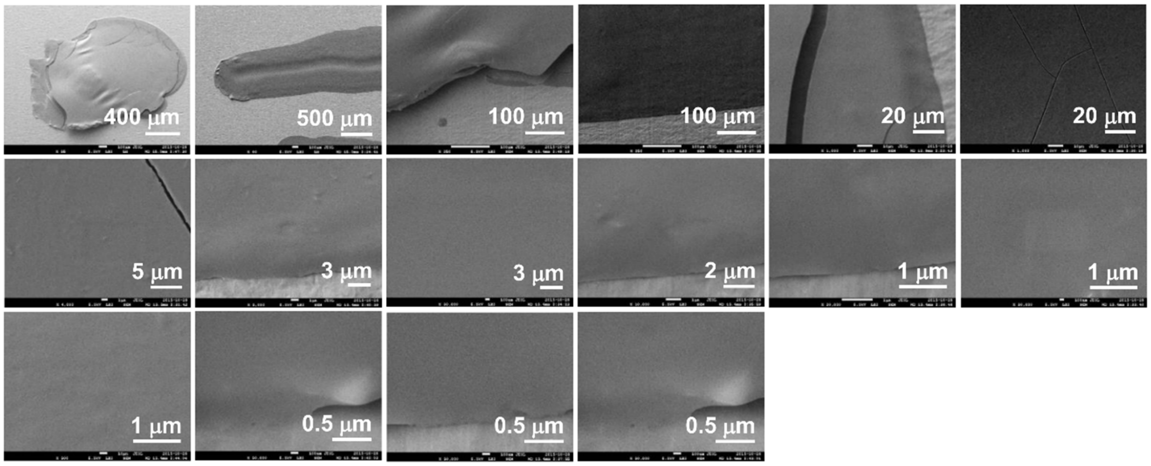

Figure S7 SEM images of the films prepared with graphene inks (2 mg.mL^{-1}, $\Gamma/\Gamma_s = 80\%$), written with a ballpoint pen on glass on aluminum foil.

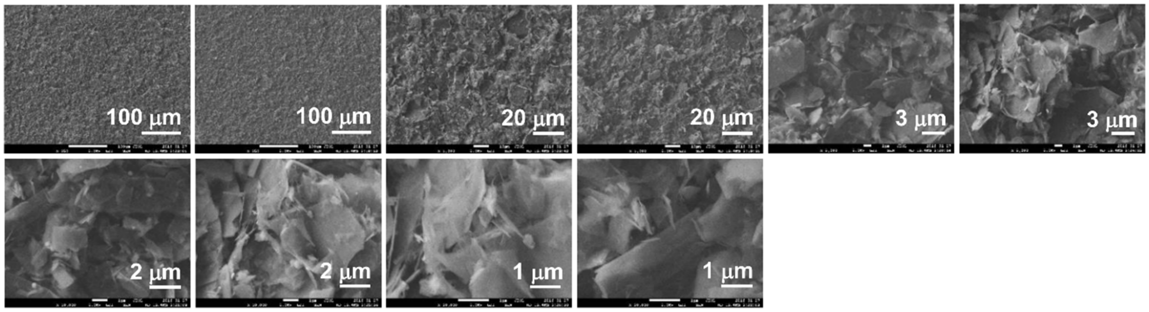

Figure S8 SEM images of the films prepared with graphene inks (0.5 mg.mL^{-1}, Γ/Γ_s = 23%) transferred to untreated glass plates via a Langmuir Blodgett transfer technique.

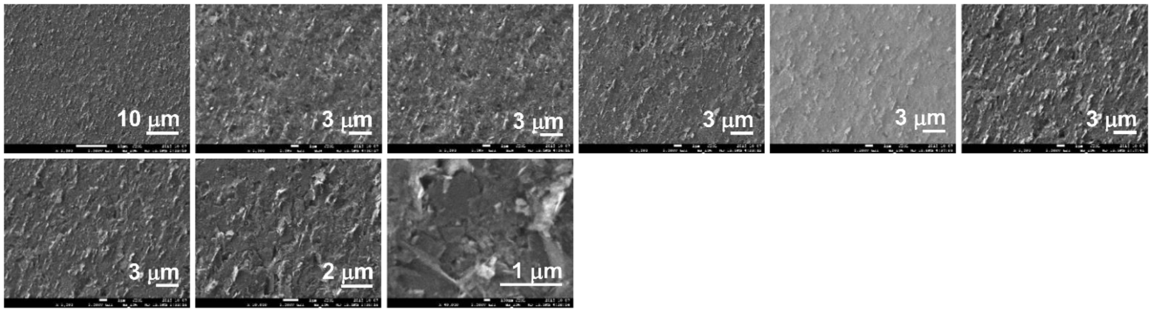

Figure S9 SEM images of the films prepared with graphene inks (1 mg.mL^{-1}, $\Gamma/\Gamma_s = 65\%$) transferred to untreated glass plates via a Langmuir Blodgett transfer technique.

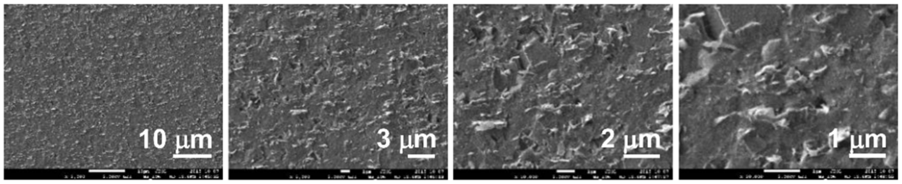

Figure S10 SEM images of the films prepared with graphene inks (2 mg.mL^{-1}, Γ/Γ_s = 80%) transferred to untreated glass plates via a Langmuir Blodgett transfer technique.

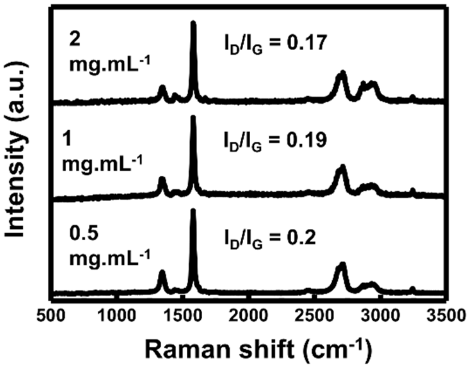

Figure S11 Raman spectrum and graphitization degree (I_D/I_G) of the films obtained by Langmuir Blodgett transfer to glass. The graphitization degree (I_D/I_G) and polymer concentration used for the preparation of the ink are indicated in the figure.

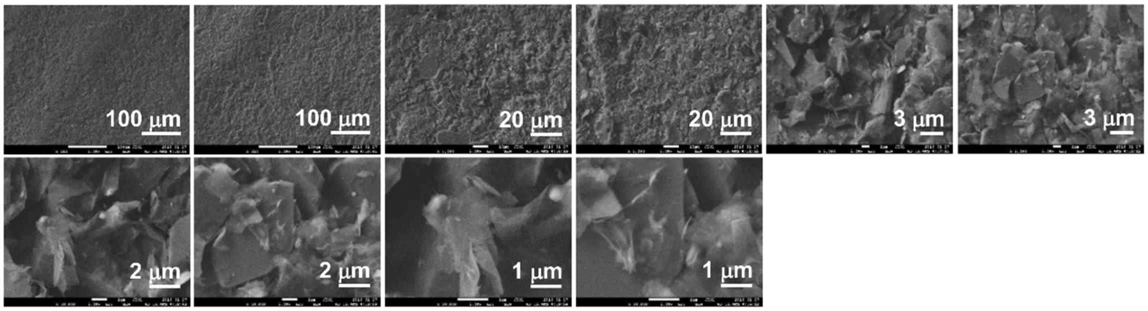

Figure S12 SEM images of the films prepared with graphene inks (0.5 mg.mL^{-1}, $\Gamma/\Gamma_s = 23\%$) transferred to HMDZ treated glass via a Langmuir Blodgett transfer technique.

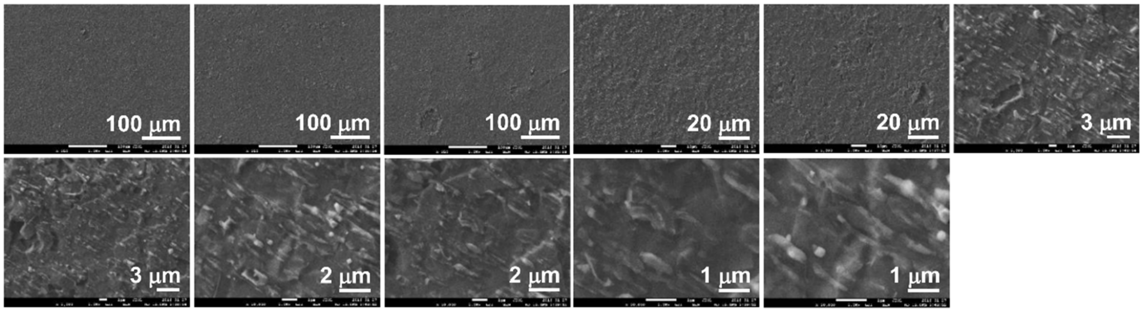

Figure S13 SEM images of the films prepared with graphene inks (0.5 mg.mL^{-1}, Γ/Γ_s = 23%) transferred to polymer treated glass via a Langmuir Blodgett transfer technique.

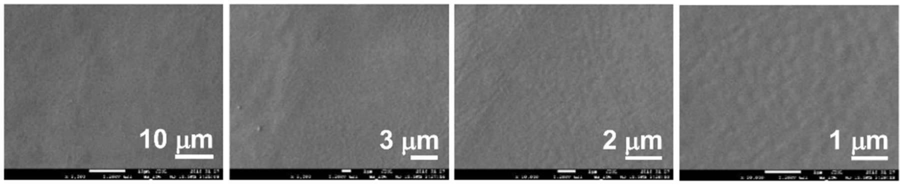

Figure S14 SEM images of the coated polymer/glass plates.

Ink drying rate measurement

To assess the ink drying rate, 50 µl of the solvent or of the ink was deposited on the ATR crystal (diamond) of the FTIR instrument, and the absorbance spectrum was saved automatically every 3 seconds. A characteristic band of the solvent is chosen to monitor the drying rate (in the case of isooctane, the band at 1450 cm^{-1} is chosen). When the band has disappeared, the ink is dried.

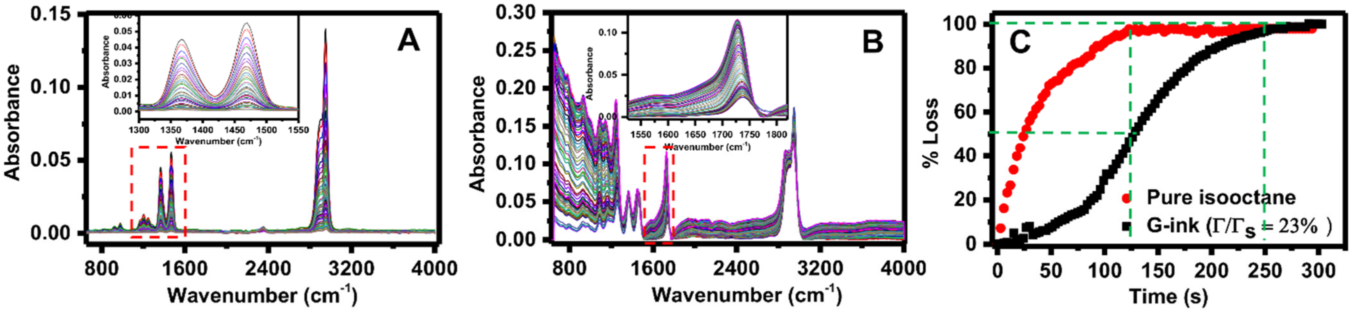

Figure S15 A. FTIR spectrum of isooctane vs time. B. FTIR spectrum of graphene ink (c = 0.5 $mgmL^{-1}$) vs time. C. %loss of the intensity of the isooctane and graphene ink vs time. At 125 s, isooctane is fully dried, while 50% of isooctane in the graphene ink was evaporated. At 250 s, the graphene ink is fully dried.

Contact angle measurements

A drop of 5 µl of isooctane was applied to a freshly cleaned glass slide, or a HMDZ treated glass slide or a polymer treated glass slides. The drop of isooctane was photographed with a digital SLR camera, and the image was analyzed using the ImageJ freeware and the Dropsnake plugin.

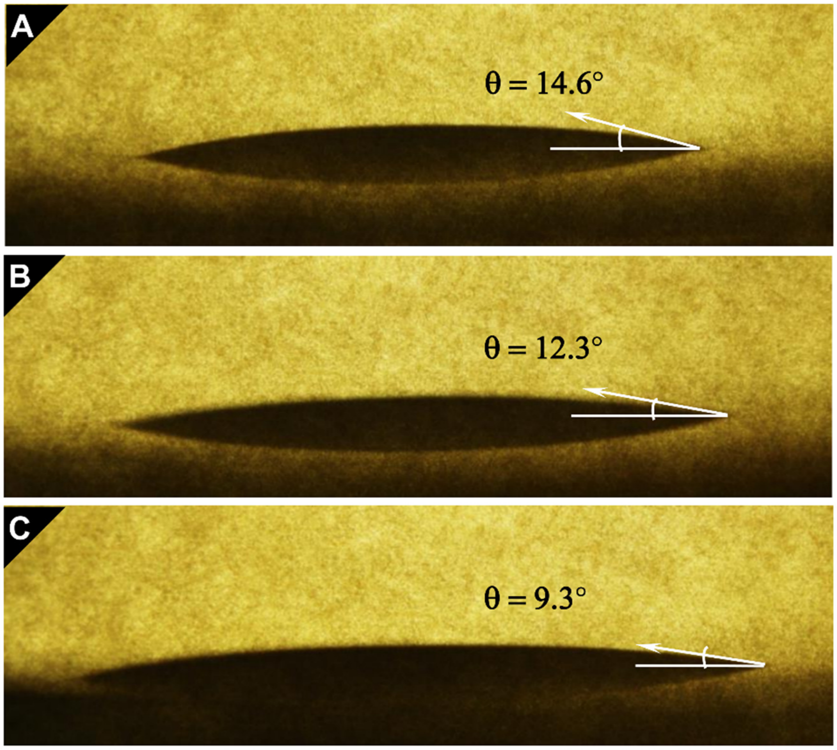

Figure S16 Contact angle of graphene ink (c = 0.5 mgmL^{-1}) with various substrates. A. untreated glass plate. B. HMDZ – treated glass plate. C. Poly(CEM$_{11}$-b-EHA$_7$) coated glass plate

Table S2 Sheet resistance R_s of films prepared with graphene inks reported in literature

	Solvent	Additive	R_s (kΩ/seq)	substrate
Torrisi *et al.*, 2012[6]	NMP	---------------	30	hexamethyldisilazane (HMDS)-treated Si wafer
Han, X. *et al.*, 2013[7]	NMP	--------	1	PET
Li, J. *et al.*, 2013[8]	terpineol	poly(ethyl cellulose) (EC)	30	Glass
Arapov *et al.*, 2014[9]	isopropanol (IPA) and n-butanol (n-BuOH)	copolymer of N-vinyl-2-pyrrolidone and vinyl acetate	1–2	FS3 and LumiForte special application papers
Ciesielski *et al.*, 2014[10]	NMP	1-phenyloctane and arachidic acid	10-25	HMDZ-treated Si wafer
Jabari et Toyserkani, 2016[11]	cyclohexanone/terpineol	----------------	0.93	HMDZ-treated Si wafers
Capasso *et al.*, 2015[12]	water/ethanol	-------------------	13	PET
Del *et al.*, 2015[13]	terpineol	EC	30	Glass slide
Higashi *et al.*, 2016[14]		p-C18-ac-2EG3	25	Filter paper
Majee, Subimal *et al.*, 2016[15]	ethanol, DMF, and NMP	EC	0.26	Glass and PET
Mousset *et al.*, 2016[16]	water/ethanol	Nafion	5.1	polytetrafluoroethylene (PTFE)-treated carbon textile

References

(1) Nguendia, J. Z.; Zhong, W.; Fleury, A.; De Grandpré, G.; Soldera, A.; Sabat, R. G.; Claverie, J. P. Supramolecular Complexes of Multivalent Cholesterol-Containing Polymers to Solubilize Carbon Nanotubes in Apolar Organic Solvents. *Chem. Asian J.* **2014**, *9*, 1356–1364.

(2) Shin, K.-Y.; Hong, J.-Y.; Jang, J. Micropatterning of Graphene Sheets by Inkjet Printing and Its Wideband Dipole-Antenna Application. *Adv. Mater.* **2011**, *23*, 2113–2118.

(3) Jeong, S. Y.; Kim, S. H.; Han, J. T.; Jeong, H. J.; Yang, S.; Lee, G. W. High-Performance Transparent Conductive Films Using Rheologically Derived Reduced Graphene Oxide. *ACS Nano* **2011**, *5*, 870–878.

(4) Gao, Y., Shi, W., Wang, W., et al. (2014). Inkjet Printing Patterns of Highly Conductive Pristine Graphene on Flexible Substrates. *Industrial & Engineering Chemistry Research*, *53*(43), 16777-16784.

(5) Li, J., Ye, F., Vaziri, S., et al. (2013). Efficient Inkjet Printing of Graphene. *Advanced Materials*, *25*(29), 3985-3992.

(6) Torrisi, F., Hasan, T., Wu, W., et al. (2012). Inkjet-printed graphene electronics. *ACS nano*, *6*(4), 2992-3006.

(7) Han, X., Chen, Y., Zhu, H., et al. (2013). Scalable, printable, surfactant-free graphene ink directly from graphite. *Nanotechnology*, *24*(20), 205304.

(8) Li, J., Ye, F., Vaziri, S., et al. (2013). Efficient Inkjet Printing of Graphene. *Advanced Materials*, *25*(29), 3985-3992.

(9) Arapov, K., Abbel, R., de With, G., et al. (2014). Inkjet printing of graphene. *Faraday Discuss.*, *173*, 323-336.

(10) Ciesielski, A., Haar, S., El Gemayel, M., et al. (2014). Harnessing the Liquid-Phase Exfoliation of Graphene Using Aliphatic Compounds: A Supramolecular Approach. *Angewandte Chemie International Edition*, *53*(39), 10355-10361.

(11) Capasso, A., Del Rio Castillo, A. E., Sun, H., et al. (2015). Ink-jet printing of graphene for flexible electronics: An environmentally-friendly approach. *Solid State Communications*, *224*, 53-63.

(12) Del, S. K., Bornemann, R., Bablich, A., et al. (2015). Optimizing the optical and electrical properties of graphene ink thin films by laser-annealing. *2D Materials*, *2*(1), 11003.

(13) Higashi, C., Funasaki, Y., Iguchi, H., et al. (2016). In situ polymerization of a novel surfactant on a graphene surface for the stable dispersion of graphene in water. *RSC Adv.*, *6*(91), 88244-88247. https://doi.org/10.1039/C6RA20315A

(14) Jabari, E. et Toyserkani, E. (2016). Aerosol-Jet printing of highly flexible and conductive graphene/silver patterns. *Materials Letters*, *174*, 40-43.

(15) Majee, S., Song, M., Zhang, S.-L., et al. (2016). Scalable inkjet printing of shear-exfoliated graphene transparent conductive films. *Carbon*, *102*, 51-57.

(16) Mousset, E., Ko, Z. T., Syafiq, M., et al. (2016). Electrocatalytic activity enhancement of a graphene ink-coated carbon cloth cathode for oxidative treatment. *Electrochimica Acta*, *222*, 1628-1641.